Australian Journal of Basic and Applied Sciences, 7(4): 78-89, 2013
ISSN 1991-8178

Unsteady Double Diffusive Magneto Hydrodynamic Boundary Layer Flow Of A Chemically Reacting Fluid Over A Flat Permeable Surface

[1]David Theuri, [2]Oluwole Daniel Makinde, [1]Nancy Wangare Kabuki

[1]Department of Pure and Applied Mathematics, Jomo Kenyatta University of Agriculture and Technology, P. O. Box 62000-00200, Nairobi, Kenya.
[2]Institute for Advanced Research in Mathematical Modelling and Computations, Cape Peninsula University of Technology, P. O. Box 652, Cape Town 8000, South Africa.

Abstract: This paper investigates the combined effects of thermal-diffusion (Soret number) and diffusion-thermo (Dufour number) on heat and mass transfer by unsteady hydromagnetic boundary layer flow of a conducting incompressible fluid over a permeable flat surface in the presence of a first order homogeneous chemical reaction. Using similarity approach, the governing equations of momentum, energy and concentration balance are transformed to a set of ordinary differential equations and tackled numerically using Newton–Raphson shooting method along with a fourth-order Runge–Kutta integration scheme. The influence of various pertinent parameters on the fluid velocity, temperature, concentration, skin friction, Nusselt number and Sherwood number are presented graphically and discussed quantitatively.

Key words: Unsteady flow; Flat permeable surface; Heat and mass transfer; Magnetic field; Dufour and Soret effects; Chemical reaction

INTRODUCTION

Studies related to double diffusive hydromagnetic boundary layer flow with heat and mass transfer over flat surfaces are extremely important and have many applications in engineering and industrial processes (Mc Dougall, T.J., J. Fluid Mech., 1982; Chamkha, A.J., 1997). For instance, heat and mass transfer occur in processes, such as drying, evaporation at the surface of a water body, and energy transfer in a wet cooling tower, cooling of nuclear reactors, magnetohydrodynamic (MHD) power generators, MHD pump, chemical vapour deposition on surfaces, formation and dispersion of fog, distribution of temperature and moisture over agriculture fields, etc. Moreover, when heat and mass transfer occur simultaneously between the fluxes, the driving potentials are of more intricate nature (Jaluria, Y., 1980; Abd El-Aziz, M., 2009; Mohamed, R.A. and S.M. Abo-Dahab, 2009). An energy flux can be generated not only by temperature gradients but by composition gradients. The energy flux caused by a composition is called Dufour or diffusion-thermo effect. Temperature gradients can also create mass fluxes, and this is the Soret or thermal-diffusion effect. The concept of Soret and Dufour effects on heat and mass transfer has been developed from the kinetic theory of gases by Chapman and Cowling (1952) and Hirshfelder *et al*. (1954). They explained the phenomena and derived the necessary formulae to calculate the thermal diffusion coefficient and the thermal-diffusion factor for monatomic gases or for polyatomic gas mixtures. The thermal-diffusion effect, for instance, has been utilized for isotope separation and in mixture between gases with very light molecular weight (Hydrogen-Hellium) and of medium molecular weight (Nitrogen-air) the diffusion-thermo effect was found to be of a magnitude such that it cannot be neglected Kafoussias and Williams (1995). Alam *et al*. (2006) studied Dufour and Soret effects on steady free convection and mass transfer flow past a semi-infinite vertical porous plate in a porous medium. Makinde (2011) studied numerically the influence of a magnetic field on heat and mass transfer by mixed convection from vertical surfaces in porous media considering Soret and Dufour effects. Makinde and Olanrewaju (2011) have investigated the Dufour and Soret effects on unsteady mixed convection flow past a porous plate moving through a binary mixture of chemically reacting fluid. The thermal diffusion and diffusion thermo effects on chemically reacting hydromagnetic boundary layer flow of heat and mass transfer past a moving vertical plate with suction /injection have been addressed by Olanrewaju and Makinde (2011).

In this present study, our objective is to analysis the effects of thermal-diffusion (Soret) and diffusion-thermo (Dufour) on heat and mass transfer by unsteady hydromagnetic first order homogeneous chemically reacting boundary layer flow over a permeable flat surface. The rest of the paper is structured as follows. In Section 2, we formulate the problem: in Section 3, the model problem is tackled numerically using shooting method with a fourth order Runge-Kutta integration scheme and the pertinent results are presented graphically and discussed quantitatively.

Corresponding Author: David Theuri, Department of Pure and Applied Mathematics, Jomo Kenyatta University of Agriculture and Technology, P. O. Box 62000-00200, Nairobi, Kenya.

2. Mathematical Model:

We consider an unsteady chemically reacting hydromagnetic flow past a stationary permeable flat plate with thermal-diffusion (Soret) and diffusion-thermo (Dufour) effects in the presence of a uniform transverse magnetic field of strength H_0. It is assumed that the induced magnetic field, the external electric field and the field due to the polarization of charges are negligible. The flow is assumed to be in the *x*-direction which is taken along the plate surface and the *y*-axis is taken normal to it as shown in figure 1. Under the boundary-layer approximations, the governing equations for continuity, momentum, energy and concentration balance can be written as (Postelnicu, A., 2004; Alam, M.S. and M.M. Rahman, 2006)

$$\frac{\partial v}{\partial y} = 0, \tag{1}$$

$$\frac{\partial u}{\partial t} + v\frac{\partial u}{\partial y} = \upsilon\frac{\partial^2 u}{\partial y^2} - \frac{\sigma {H_0}^2}{\rho}(u - U), \tag{2}$$

$$\frac{\partial T}{\partial t} + v\frac{\partial T}{\partial y} = \alpha\frac{\partial^2 T}{\partial y^2} + \frac{\upsilon}{c_p}(\frac{\partial u}{\partial y})^2 + \frac{\sigma {H_0}^2}{\rho c_p}(u - U)^2 + \frac{D_m k_T}{c_s c_p}\frac{\partial^2 C}{\partial y^2}, \tag{3}$$

$$\frac{\partial C}{\partial t} + v\frac{\partial C}{\partial y} = D_m\frac{\partial^2 C}{\partial y^2} + \frac{D_m k_T}{T_m}\frac{\partial^2 T}{\partial y^2} - \gamma(C - C_\infty), \tag{4}$$

The boundary conditions for this model are;

$$u = 0, T = T_w, C = C_w \text{ on } \quad y = 0 \tag{5}$$

$$u = U, v = 0, T = T_\infty, C = C_\infty \text{ as } y \to \infty \tag{6}$$

where (*u, v*) are the velocity components in the *x* and *y* directions respectively, υ is the kinematic viscosity, ρ is the density, *U* is the free stream velocity, *T* is the temperature, T_w is the plate surface temperature, T_∞ is the free stream temperature, *C* is the chemical species concentration, C_w is the chemical species concentration, C_∞ is the free stream concentration, α is the thermal diffusivity, D_m is the coefficient of mass diffusivity, c_p is the specific heat at constant pressure, T_m is the mean fluid temperature, γ is the first order homogenous reaction rate, k_T is the thermal diffusion ratio, and c_s is the concentration susceptibility. From equation (1), *v* is either constant or a function of time. Following Makinde (Makinde, O.D., 2005), we choose

$$v = -b\left(\frac{\upsilon}{t}\right)^{\frac{1}{2}}, \tag{7}$$

where $b > 0$ is the suction parameter. We introduce similarity variables and the dimensionless quantities, i.e.

$$\eta = \frac{y}{2\sqrt{\upsilon t}}, u = Uf(\eta),\ \theta = \frac{T - T_\infty}{T_w - T_\infty},\ \phi = \frac{C - C_\infty}{C_w - C_\infty},$$
$$\Pr = \frac{\upsilon}{\alpha}, Sc = \frac{\upsilon}{D_m}, \lambda = \frac{\gamma 4\upsilon t}{D_m}, Du = \frac{D_m k_T (C_w - C_\infty)}{c_s c_p \alpha (T_w - T_\infty)}, \tag{8}$$
$$Sr = \frac{D_m k_T (T_w - T_\infty)}{\alpha T_m (C_w - C_\infty)}, M = \frac{4t\sigma H_0^2}{\rho}, Ec = \frac{U^2}{c_p (T_w - T_\infty)}.$$

Substituting equation (7) into equations (2)-(6), we obtain

$$f'' + 2(\eta + b)f' - M(f - 1) = 0, \tag{9}$$

$$\theta'' + 2\Pr(\eta + b)\theta' + Du\phi'' + \Pr Ec(f')^2 + \Pr EcM(f - 1)^2 = 0, \tag{10}$$

$$\phi'' + 2Sc(\eta + b)\phi' + Sr\theta'' - \lambda\phi = 0, \tag{11}$$

with the boundary conditions

$$f(0) = 0, \quad \theta(0) = 1, \quad \phi(0) = 1, \tag{12}$$

$$f(\infty) = 1, \quad \theta(\infty) = 0, \quad \phi(\infty) = 0, \tag{13}$$

where *Pr* is the Prandtl number, *Sc* is the Schmidt number, *Sr* is the Soret number, *Du* is the Dufour number, *M* is the magnetic field parameter, *Ec* is the Eckert number and λ is the reaction rate parameter. The prime symbol indicates derivative with respect to η. The parameters of engineering interest for the present

problem are the local skin-friction coefficient (C_f), the local Nusselt number (Nu) and the local Sherwood number (Sh), which are given respectively by the following expressions,

$$C_f = \frac{2t\tau_w}{\rho U\sqrt{\upsilon t}} = f'(0), \tag{14}$$

$$Nu = \frac{2q_w\sqrt{\upsilon t}}{k(T_w - T_\infty)} = -\theta'(0), \tag{15}$$

$$Sh = \frac{2S_w\sqrt{\upsilon t}}{D_m(C_w - C_\infty)} = -\phi'(0), \tag{16}$$

where the τ_w, q_w and S_w are the local shear stress, local heat transfer rate and local mass transfer rate at the place surface respectively. They are given as

$$\tau_w = \rho\upsilon\left.\frac{\partial u}{\partial y}\right|_{y=0}, \quad q_w = -k\left.\frac{\partial T}{\partial y}\right|_{y=0}, \quad S_w = -D_m\left.\frac{\partial C}{\partial y}\right|_{y=0}, \tag{17}$$

where k is the fluid thermal conductivity coefficient.

3. Numerical Procedure:

The set of equations (9)–(11) under the boundary conditions (12)-(13) have been solved numerically using Newton–Raphson shooting method along with a fourth-order Runge–Kutta integration algorithm, Na [16]. Let

$$f = x_1,\ f' = x_2,\ \theta = x_3,\ \theta' = x_4,\ \phi = x_5,\ \phi' = x_6. \tag{18}$$

Equations (9)-(11) then reduced to a system of first order differential equations as:

$$\begin{aligned}
x_1' &= x_2,\\
x_2' &= M(x_1 - 1) - 2(\eta + b)x_2,\\
x_3' &= x_4,\\
x_4' &= \frac{2ScDu(\eta + b)x_6 - Du\lambda x_5 - 2\,\mathrm{Pr}(\eta + b)x_4 - \mathrm{Pr}\,Ecx_2^2 - \mathrm{Pr}\,EcM(x_1 - 1)^2}{(1 - DuSr)},\\
x_5' &= x_6,\\
x_6' &= \frac{\lambda x_3 + 2\,\mathrm{Pr}\,Sr(\eta + b)x_4 + \mathrm{Pr}\,SrEcx_2^2 + \mathrm{Pr}\,SrEcM(x_1 - 1)^2 - 2Sc(\eta + b)x_6}{(1 - DuSr)},
\end{aligned} \tag{19}$$

subject to the following initial conditions;

$$x_1(0) = 0,\ x_2(0) = s_1,\ x_3(0) = 1,\ x_4(0) = s_2,\ x_5(0) = 1,\ x_6(0) = s_3. \tag{20}$$

The unspecified initial conditions s_1, s_2 and s_3 are guessed systematically and the system in equation (19) is then integrated numerically as initial valued problems to a given terminal point. The procedure was repeated until the results attained the desired degree of accuracy, namely 10^{-7}. The value of η_∞ was found for each iteration loop by the assignment statement $\eta_\infty = \eta_\infty + \Delta\eta$. The maximum value of η_∞ to each group of parameters M, Pr, Du, Sr, Sc, b, Ec, λ was determined when the values of unknown boundary conditions at η = 0 did not change in successive loops with error more than 10^{-7}. From the process of numerical computation (Heck 2003), the local skin-friction coefficient, the local Nusselt number and the local Sherwood number in equations (14)-(16) are also worked out and their numerical values are presented graphically.

RESULTS AND DISCUSSION

Figures 2-20 illustrate the computational results showing the effects of various thermophysical parameters on the electrically conducting and first order homogeneous reacting fluid velocity, temperature, concentration as well as heat and mass transfer over a permeable flat surface. The Prandtl number was taken to be Pr = 0.71, which corresponds to air and the values of Schmidt number (Sc) were chosen to be Sc = 0.24, 0.6, 0.78, 2.62, representing diffusing chemical species of most common interest in air like H_2, H_2O, NH_3 and Propyl Benzene respectively. The values of Soret number Sr and Dufour number Du are chosen in such a way that their product

is constant according to their definition provided that the mean temperature T_m is kept constant, Kafoussias and Williams (1995). These values are used throughout the computations, unless otherwise indicated.

Table 1: Computations showing the effects of thermophysical parameters on C_f, Nu, Sh.

M	b	Du	Sr	Sc	Ec	λ	C_f	Nu	Sh
0	0.1	0.4	0.15	0.6	0.1	0.1	1.258709	0.797161	0.944878
0.1	0.1	0.4	0.15	0.6	0.1	0.1	1.296189	0.794290	0.945287
1	0.1	0.4	0.15	0.6	0.1	0.1	1.600921	0.770977	0.948626
1	0.5	0.4	0.15	0.6	0.1	0.1	2.137117	1.031449	1.240412
1	1	0.4	0.15	0.6	0.1	0.1	2.897463	1.390006	1.643774
1	-0.5	0.4	0.15	0.6	0.1	0.1	0.959879	0.440371	0.578890
1	-1	0.4	0.15	0.6	0.1	0.1	0.600423	0.234788	0.346687
1	0.1	1	0.06	0.6	0.1	0.1	1.600921	0.433448	0.995798
1	0.1	2	0.03	0.6	0.1	0.1	1.600921	-0.129101	1.011522
1	0.1	0.4	0.15	0.24	0.1	0.1	1.600921	0.875718	0.582798
1	0.1	0.4	0.15	0.78	0.1	0.1	1.600921	0.723904	1.098049
1	0.1	0.4	0.15	2.62	0.1	0.1	1.600921	0.334487	2.213978
1	0.1	0.4	0.15	0.6	0.5	0.1	1.600921	0.470899	0.990067
1	0.1	0.4	0.15	0.6	1	0.1	1.600921	0.095801	1.041868
1	0.1	0.4	0.15	0.6	0.1	0.5	1.600921	0.703204	1.143402
1	0.2	0.4	0.15	0.6	0.1	1	1.600921	0.628805	1.354634

A. Velocity Profiles:

Generally, the conducting fluid velocity is zero at the fixed plate surface, and then increases until the free stream prescribed value is attains, satisfying the far field boundary condition. In figure 2, we observed that an increase in the magnetic field intensity (M) pushes the fluid towards the plate surface, leading to a decrease in the momentum boundary layer thickness. The presence of magnetic field in an electrically conducting reacting fluid introduces a force called the Lorentz force, which acts against the flow if the magnetic field is applied in the normal direction, as in the present problem. This type of resisting force slows down the fluid velocity as shown in this figure. Figures 3 and 4 illustrate the effects of increasing suction and injection on the reacting fluid velocity profiles. As the fluid suction increases ($b > 0$), the momentum boundary layer thickness decreases and the fluid push towards the permeable plate surface. The trend of the velocity profiles for the case of injection ($b < 0$) is opposite. The momentum boundary layer increases with increasing fluid injection. These results are in perfect agreement with the earlier results reported by Afify (2009) on the effects of suction / injection on the MHD boundary layer flow over a stretching surface.

B. Temperature Profiles:

Figures 5-10 represent the graph showing the effects of various thermophysical parameters on the temperature distribution. It is noteworthy that, the temperature is maximum at the permeable plate surface and asymptotically decreases to zero far away from the plate satisfying the boundary condition. An increase in the magnetic field intensity parameter M as demonstrated in figure 5, causes the reacting conducting fluid temperature to overshoot towards the permeable plate surface leading to further increase in the reacting fluid temperature within the boundary layer region. This can be attributed to the presence of Ohmic heating due to magnet field. In figures 6-7, we observed that the thermal boundary layer thickness decreases with an increase in suction ($b >0$) and increases with an increase in injection ($b < 0$). Figures 8-9 illustrates the effects of increasing Schmidt number Sc and Dufour number Du on the reacting fluid temperature. It is noteworthy that the fluid temperature increases with increasing values of Schmidt number and Dufour number Du due to a decrease in the reacting species molecular diffusivity and an increase in diffusion-thermo effects. This invariably leads to a further thickening of the thermal boundary layer. Similar trend is observed in figure 10 with increasing Eckert number Ec due to viscous dissipation effect. As the Eckert number increases, the reacting fluid temperature overshoots toward the plate surface and a general increase in the thermal boundary layer thickness occur.

C. Concentration Profiles:

The reacting chemical species concentration profiles against spanwise coordinate η for varying values of physical parameters in the boundary layer are demonstrated in figures 11-15. Generally, the concentration of the reacting chemical species is highest at the plate surface and decreases asymptotically to the prescribed free stream value, satisfying the far field boundary condition. The thermal-diffusion (Soret) effect on the concentration profiles is illustrated in figure 11. It is clearly observed from this figure that the concentration boundary layer increases with increasing value of Soret number Sr. In figures 12-13, an increase in the fluid injection ($b < 0$) causes an increase in the solutal boundary layer thickness while an increase in the fluid suction ($b > 0$) at the place surface decreases the solutal boundary layer thickness. The effect of Schmidt number Sc on concentration profiles is depicted in figure 14. An increase in the Schmidt number Sc decreases the

concentration boundary layer thickness, leading to a reduction in the reacting species concentration profiles. As *Sc* increases, the reacting species molecular diffusion *D* decreases. For diffusing chemical species in air with very light or medium molecular weight like H_2, H_2O, NH_3 and Propyl Benzene under consideration, the concentration boundary layer thickness for H_2 is the largest, followed by H_2O, NH_3, while Propyl Benzene produced the thinnest concentration boundary layer. It can be seen from figure 15 that the concentration of the fluid decreases with the increase in the destructive first order homogeneous reaction rate parameter λ.

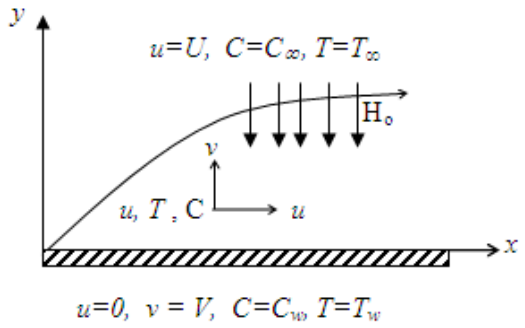

Fig. 1: Flow configuration and coordinate system

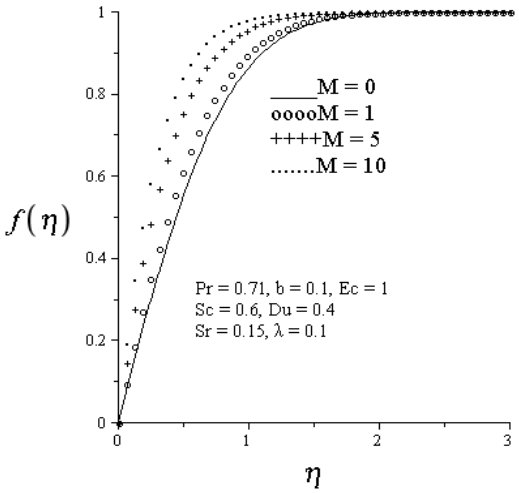

Fig. 2: Effect of magnetic field on the velocity profiles

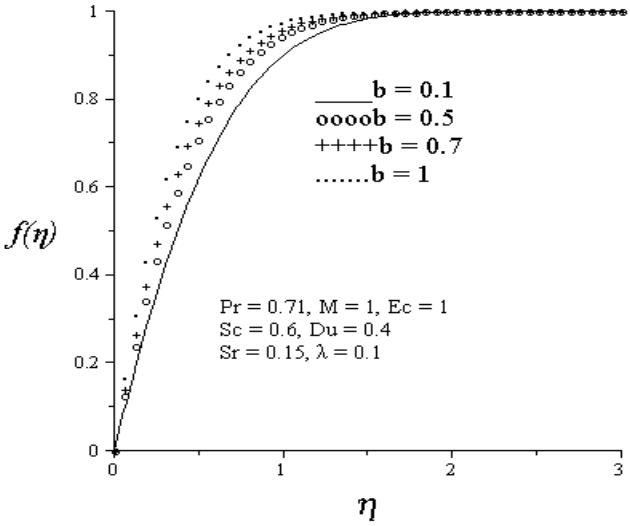

Fig. 3: Effect of fluid suction on the velocity profiles

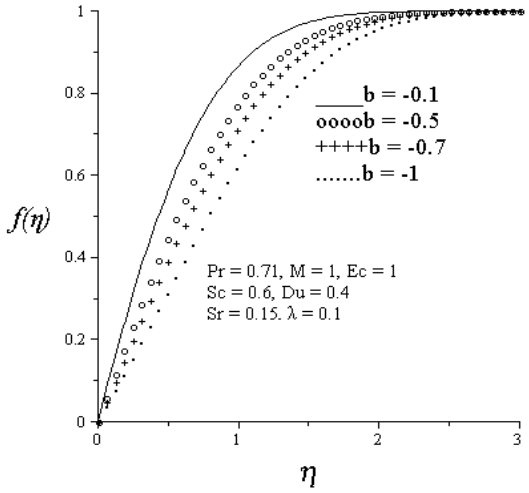

Fig. 4 : Effect of fluid injection on the velocity profiles

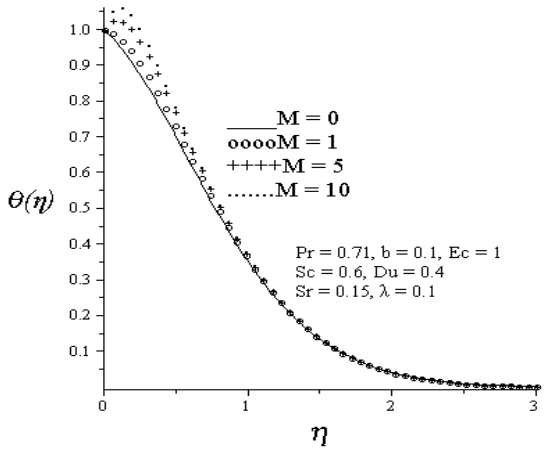

Fig. 5: Effect of magnetic field on the temperature profiles

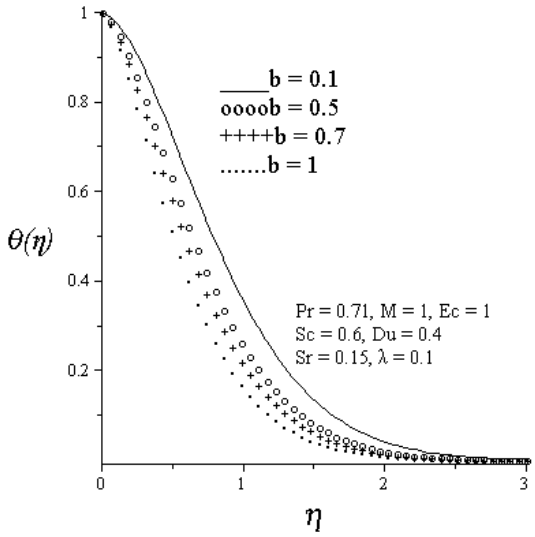

Fig. 6: Effect of fluid suction on the temperature profiles

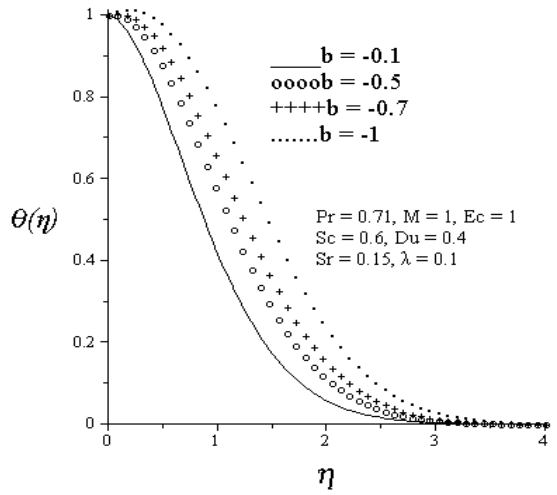

Fig. 7: Effect of fluid injection on the temperature profiles

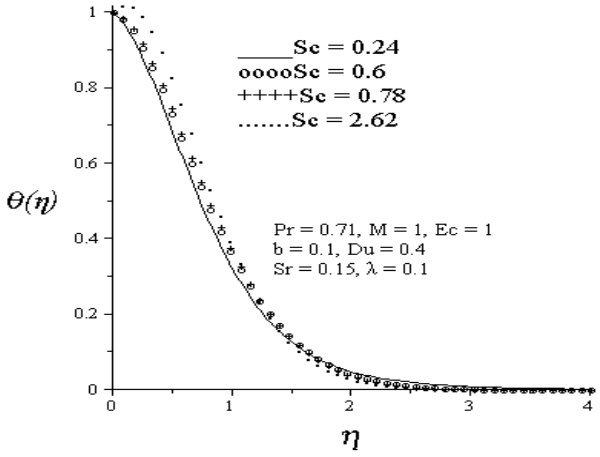

Fig. 8: Effect of increasing Sc on the temperature profiles

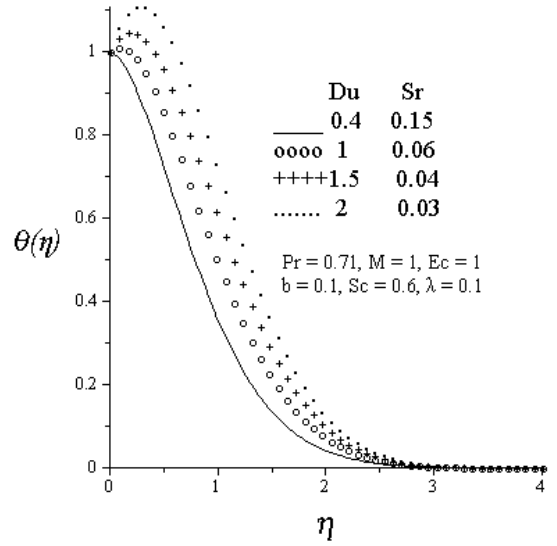

Fig. 9: Effects of *Du* and *Sr* on the temperature profiles

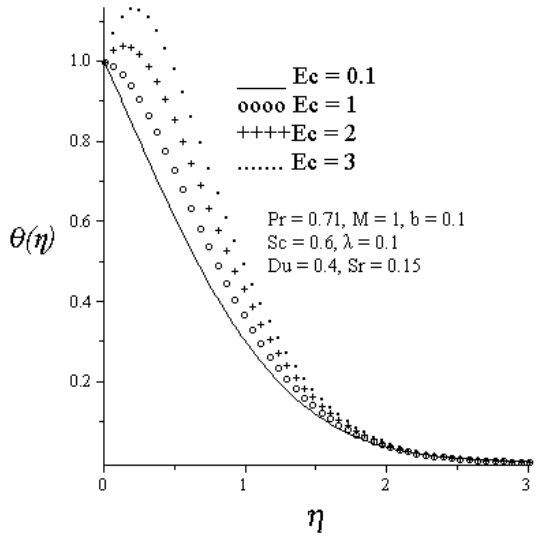

Fig. 10: Effect of *Ec* on the temperature profiles

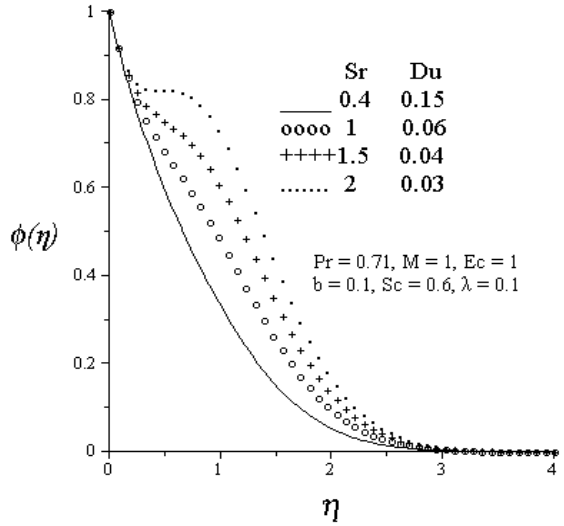

Fig. 11: Effects of *Du* and *Sr* on the concentration profiles

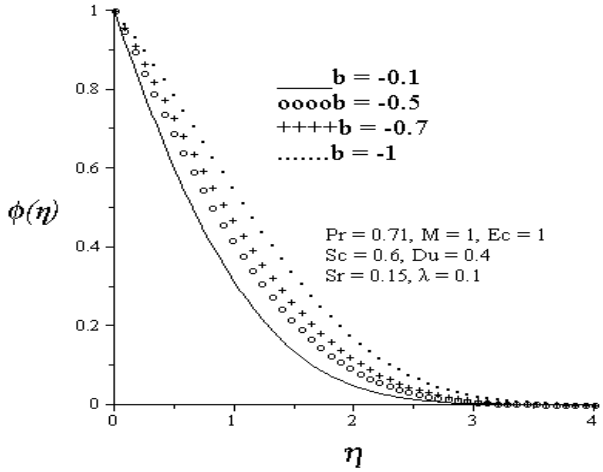

Fig. 12: Effect of fluid injection on the concentration profiles

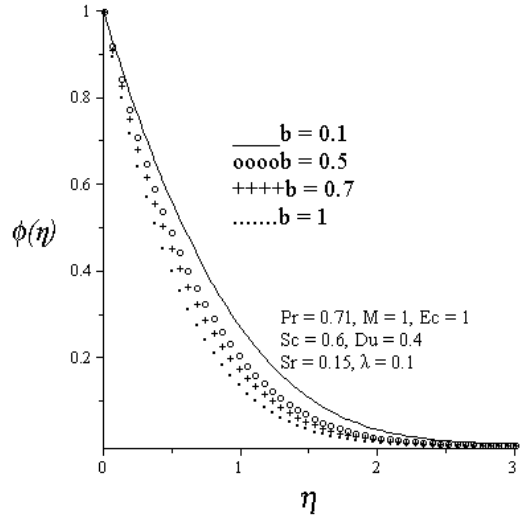

Fig. 13: Effect of fluid suction on the concentration profiles

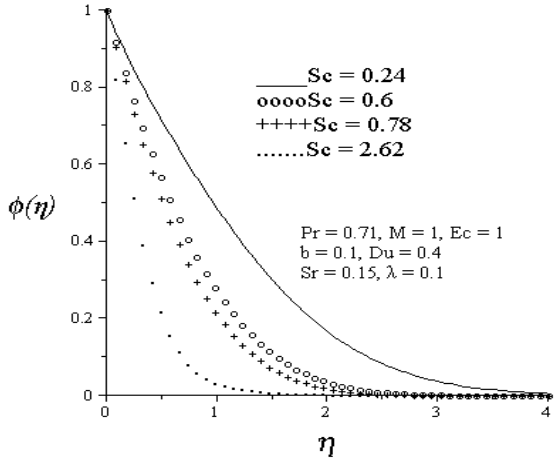

Fig. 14: Effect of increasing Schmidt number on the concentration profiles

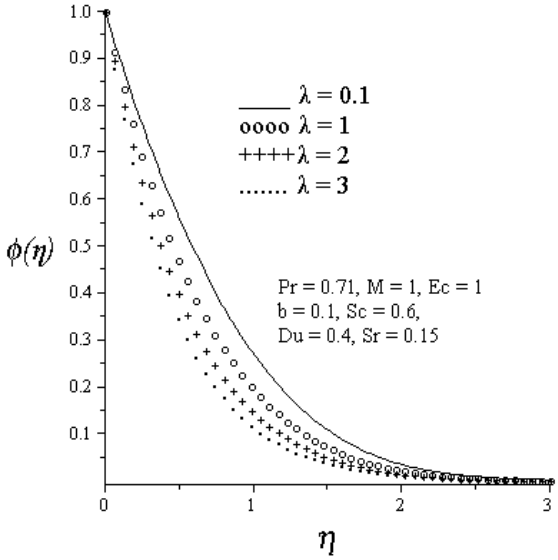

Fig. 15: Effect of increasing reaction rate on the concentration profiles

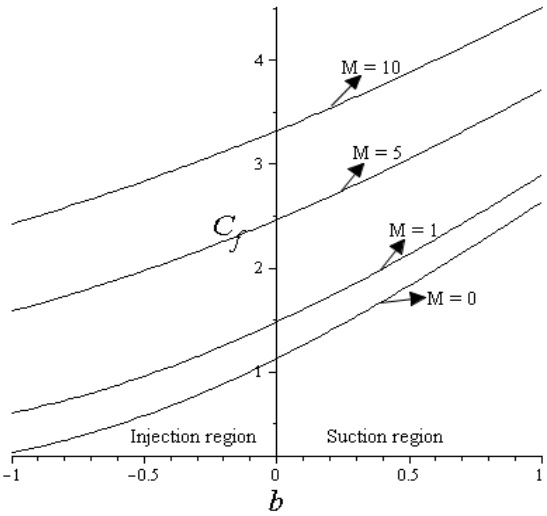

Fig. 16: Skin friction profiles with parameter variation

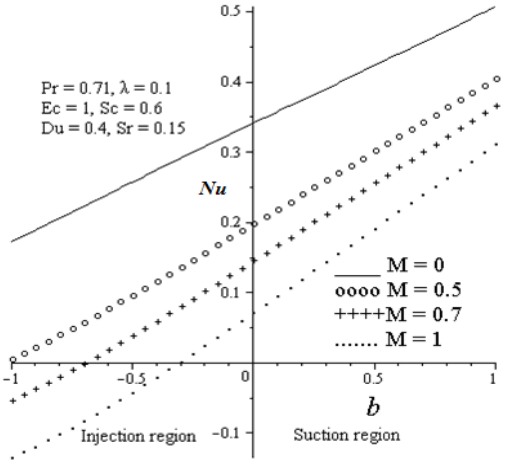

Fig. 17: Effects of magnetic field and suction/injection on Nusselt number

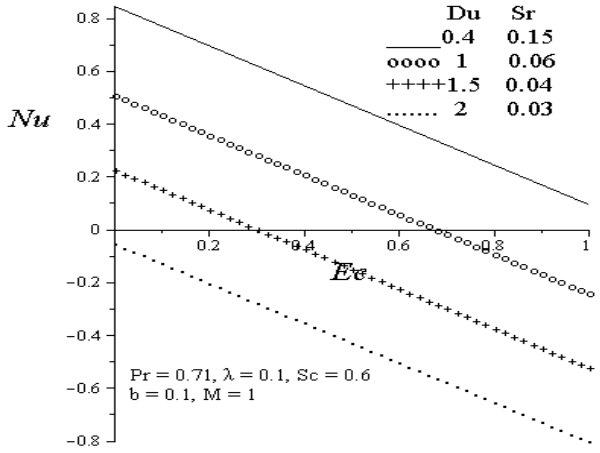

Fig. 18: Effects of Du, Sr and Ec on Nusselt number

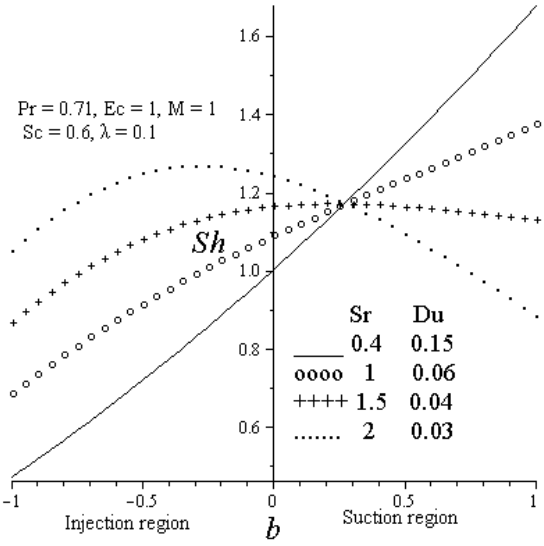

Fig. 19: Effects of increasing suction/injection and Soret number on Sherwood number

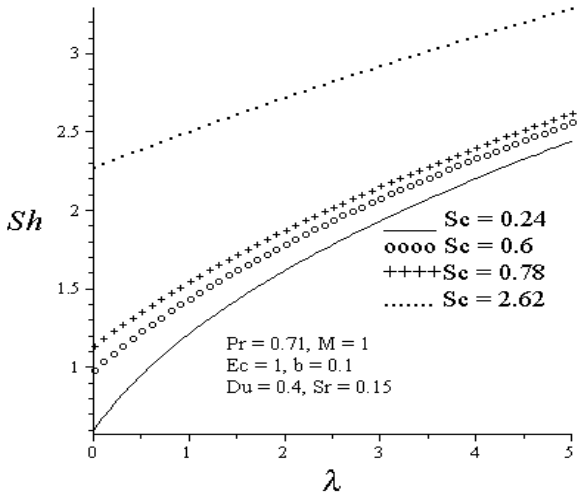

Fig. 20: Effect of increasing reaction rate and Schmidt number on Sherwood number

D. Skin friction, Nusselt number and Sherwood number:

Figures 16- 20 together with table 1 illustrate the effects of parameter variations on skin friction, heat and mass transfer at the plate surface. The shear stress at the plate surface increases with suction and decreases with injection as depicted in figure 16. It is interesting to note that an increase the magnetic field intensity M causes a further increase in the skin friction. It can be observed from figure 17 that the rate of heat transfer at the plate surface represented by the Nusselt number Nu increases with increasing fluid suction and decreases with increasing fluid injection and magnetic field intensity. This can be attributed to the fact that as the magnetic field intensity increases, the plate surface temperature increases due to Ohmic heating, leading to a decrease in the temperature gradient at the place surface. It is observed from figure 18 that Nusselt number decreases with increasing values of the Dufour number Du and Eckert number Ec. As Du and Ec increase, place surface temperature is enhanced due to a combined action of diffusion-thermo effect and viscous heating, leading to a decrease in the temperature gradient at the plate surface. This agreed with the earlier results reported by Alam and Rahman (Alam, M.S. and M.M. Rahman, 2006). Figure 19 displays the mass transfer rate at the plate surface for different values of Soret number Sr and suction/injection parameter b. It can be observed from this figure that the Sherwood number Sh increases with the increase in fluid suction ($b > 0$) and decreases with the increase in fluid injection ($b < 0$). Meanwhile, an increase in Soret number Sr due to thermo-diffusion effect enhances the mass transfer rate at the plate surface during injection ($b < 0$). For very small value of fluid suction parameter ($b > 0$), the Sherwood number Sh increases with increasing Soret number Sr. As the fluid suction

intensifies, the Sherwood number *Sh* decreases with increasing Soret number *Sr*. It is interesting to note that at suction parameter value *b* (= 0.25) the Sherwood number *Sh* (= 1.17) is not affected with increasing value of Soret number *Sr*. Figure 20 elucidates that increases in Schmidt number Sc increase the mass transfer rate at the plate surface. Similar trend is observed with increasing rate of destructive chemical reaction, the Sherwood number *Sh* increases with increasing value of λ.

Conclusions:

Numerical solutions are obtained for combined effects of thermal-diffusion (Soret) and diffusion-thermo (Dufour) on heat and mass transfer by unsteady hydromagnetic boundary layer flow of a conducting fluid over a permeable flat surface in the presence of a first order homogeneous chemical reaction. In the light of the present investigation, the following conclusions can be drawn:

- The momentum boundary layer thickness decreases with suction and increases with injection.
- The fluid velocity pushes toward the plate surface as the magnetic field intensity increases.
- The thermal boundary layer thickness increases with increasing injection, magnetic field intensity, Eckert number, Dufour number and decreases with increasing fluid suction.
- The concentration boundary layer thickness decreases with increasing suction, Schmidt number, reaction rate and increases with increasing injection, Soret number.
- The skin friction increases with increasing suction and magnetic field, and decreases with increasing injection.
- The Nusselt number decreases with increasing injection, Dufour number, magnetic field intensity, Eckert number, and increases with increasing suction.
- The Sherwood number increases with increasing suction, Schmidt number, reaction rate and decreases with injection.
- With injection, the Sherwood number increases with increasing Soret number. At suction parameter value *b*(=0.25) Sherwood number *Sh* (= 1.17) is not affected with increasing Soret number.

REFERENCES

Abd El-Aziz, M., 2009. Phy. Let. Section A, 372(3): 263.

Afify, A.A., 2009. Comm. Nonlinear Sci. Num. Simulat., 14(5): 2202.

Alam, M.S. and M.M. Rahman, 2006. Nonlinear Analy. Model. Cont., 11: 3.

Alam, M.S., M. Ferdows, M. Ota and M. A. Maleque, 2006. Int. J. Appl. Mech. Eng., 11(3): 535.

Chamkha, A.J., 1997. Int. J. Eng. Sci. 37, 975.

Chapman, S. and T.G. Cowling, 1952. The Mathematical Theory of non-Uniform Gases, Cambridge Univ. Press, Cambridge UK.

Heck, A., 2003. Introduction to Maple, 3rd Edition, Springer-Verlag.

Hirshfelder, J.O., C.F. Curtis and R.B. Bird, 1954. Molecular Theory of Gases and Liquids, Wiley, New York.

Jaluria, Y., 1980. Natural Convection Heat and Mass Transfer, Pergamon Press, Oxford, UK.

Kafoussias, N.G. and E.W. Williams, 1995. Int. J. Eng. Sci. 33: 1369.

Makinde, O.D. and P.O. Olanrewaju, 2011. Chem. Eng. Comm., 198(7): 920.

Makinde, O.D., 2005. Int. Comm. Heat Mass Trans., 32: 1411.

Makinde, O.D., 2011. Latin Amer. Appl. Res., 41: 63.

Mc Dougall, T.J., J. Fluid Mech., 1982. 126: 379.

Mohamed, R.A. and S.M. Abo-Dahab, 2009. Int. J. Thermal Sci. 48: 1800.

Na, T.Y., 1979. Computational Methods in Engineering Boundary Value Problems, Academic Press, New York.

Olanrewaju, P.O. and O.D. Makinde, J. Arabian, 2011. Sci. Eng., 36: 1607.

Postelnicu, A., 2004. Int. J. Heat Mass Trans. 47: 1467.